Microfluidic platforms for characterization of crude oil emulsion stability

Ghasemi, Homa; Mozaffari, Saeed; Mohammadghasemi, Hossein; Jemere, Abebaw B.; Nazemifard, Neda

Publisher's version / Version de l'éditeur:
https://doi.org/10.1139/cjc-2021-0248
Canadian Journal of Chemistry, 100, 7, pp. 484-494, 2022-03-30

Canadian Science Publishing | Canadian Journal of Chemistry

Microfluidic Platform for Characterization of Crude Oil Emulsion Stability

Journal:	*Canadian Journal of Chemistry*
Manuscript ID	Draft
Manuscript Type:	Mini Review
Date Submitted by the Author:	n/a
Complete List of Authors:	Ghasemi, Homa; University of Wisconsin-Milwaukee, Department of Materials Science & Engineering Mozaffari, Saeed; Virginia Polytechnic Institute and State University, Department of Chemical Engineering; University of Alberta, Department of Chemical and Materials Engineering Mohammadghasemi, Hossein; University of Tehran Jemere, Abebaw B.; National Research Council Canada Nanotechnology Research Centre Nazemifard, Neda; University of Alberta, Department of Chemical and Materials Engineering
Is the invited manuscript for consideration in a Special Issue? :	UofA Analytical special issue
Keyword:	Microfluidics, Crude Oil Emulsions, Coalescence, Interfacial Elasticity, Asphaltenes

Microfluidic Platform for Characterization of Crude Oil Emulsion Stability

Homa Ghasemi[a], Saeed Mozaffari[b, c,*], Hossein Mohammadghasemi[d], Abebaw B. Jemere[e], Neda Nazemifard[c,*]

[a] Department of Materials Science & Engineering, College of Engineering & Applied Science, University of Wisconsin-Milwaukee, Milwaukee 53211, USA

[b] Department of Chemical Engineering, Virginia Polytechnic Institute and State University, Blacksburg, VA 24060, USA

[c] Department of Chemical and Materials Engineering, University of Alberta, Edmonton, T6G 2V4 AB, Canada

[d] School of Chemical Engineering, College of Engineering, University of Tehran, Tehran, Iran

[e] National Research Council Canada – Nanotechnology Research Centre, Edmonton, T6G 2M9, AB, Canada

* Corresponding authors: nn1@ualberta.ca ; saeedm6@vt.edu

ABSTRACT

Microfluidic technology has gained significant scientific interest in characterization of crude oil emulsions often formed during oil production. Microfluidic platforms can be used to mimic the pores of natural rocks and further study the multiphase displacements as well as emulsion formation at a microscale geometry. This mini-Review focuses on the applications of microfluidics to probe the stability of emulsified droplets against coalescence (e.g., in the presence of additives, electric field, etc.) for both water-in-oil (W/O) and oil-in-water (O/W) emulsion systems. Additionally, this study summarizes the recent efforts made to identify the effects of various experimental factors, including crude oil composition, aging, salinity, and pH on the interfacial properties of water/oil interface and their ultimate roles in the formation/stability of emulsions. Finally, main findings and some recommendations for future work related to the potential of microfluidics in different aspects of crude oil emulsion studies are provided.

Keywords: Microfluidics, Oil Production, Crude Oil Emulsions, Demulsifiers, Asphaltenes, Coalescence, Salinity, and Interfacial Elasticity

INTRODUCTION

Microfluidics is a unique technology, which deals with the fluid flow at the microscale. Microfluidic platforms consist of channels with dimensions of 10-100 μm, which manipulate 10^{-9} to 10^{-18} L amounts of fluids[1]. The miniaturized systems allow for significant reduction in the sample volume and aid with rapid screening of materials properties. Microfluidics has different applications in chemical, biological, biochemical, and industrial processes[2, 3] and can be found in the literature with different names, such as microreactors and lab-on-a-chip[4, 5]. Broad range of materials including glass[6, 7], polymers such as polydimethylsiloxane (PDMS)[8, 9], poly(methyl methacrylate) (PMMA)[10], and ceramics[11] were used to fabricate these miniaturized devices. Microfluidic systems have been extensively used to probe different properties of emulsion systems (e.g., stability, phase separation, interfacial elasticity) due to their time efficiency, on-site analysis ability to create prototypes efficiently; health and safety benefits[3, 12]. Recently, the applications of microfluidics have been extended to crude oil and natural gas systems as they could provide key information regarding the stability mechanism of crude oil emulsions[3, 13, 14]. Crude oil emulsions can be formed at many stages such as drilling, transportation, and crude oil recovery process[15]. Additionally, the emulsification can occur at different locations, such as reservoirs, wellbores, choke valves, surface facilities, and refineries[16]. Presence of water, enough shear force and some inorganic solids, such as sand or clay result in the formation of stable emulsion during the oil recovery processes[17-22]. Additionally, in some cases formation of multiple emulsions of water-oil-water (W/O/W) and oil-water-oil (O/W/O) adds to complexity of recovery process[16]. Generally, formation of stable emulsions (e.g., W/O) lowers the oil dehydration rate during primary processing, accelerates the corrosion rate due to their high salt content, and increases the risk of downstream separation[23-25]. These emulsions are difficult to separate due to the presence of indigenous surface-active agents and fine particles like clay and asphaltenes at the water/oil interface.

There are several procedures involved in the separation of water and oil based on the droplet size such as gravity separation, hydrocyclone or gas flotation (mostly for larger droplets), and separation by adding additives[13]. All these traditional W/O separation principle is based on the droplet growth and coalescence which can be depicted in three different stages: (i) droplet collision, (ii) thin film drainage and (iii) film rupture and subsequent coalescence of small droplets to form larger ones[26]. However, as already mentioned the presence of different surface-active agents and fine particles would slow down the coalescence kinetics of emulsified droplets as they change the properties of water/oil interface[27, 28]. Additionally, the water salinity, crude oil composition, pH, and aging the interface could have drastic effects on the interfacial properties (e.g., elasticity)[13, 29].

Microfluidic platforms containing networks of pores and pore throats are excellent models for porous media observed in the natural rocks. These micromodels allow for direct visualization of fluid flow at the length scales comparable to the reservoir pore sizes and have great potential in probing the interfacial properties of water/crude oil emulsion systems.

This mini-Review presents recent developments in understanding the stabilization/destabilization of crude oil emulsions including both water-in-oil (W/O) and oil-in-water (O/W) with the aid of various microfluidic systems. This study highlights the importance of using microfluidics to obtain key information on the interfacial properties of water/oil interface and pore-level displacement events. The application of microfluidics in probing the interfacial elasticity of crude oil-brine is discussed in detail. Finally, main findings and some recommendations for future work related to the applications of microfluidics to different aspects of crude oil emulsion studies, including interfacial rheology and coalescence kinetics of emulsified droplets are presented.

Microfluidics investigation of water-in-crude oil emulsions (W/O) stability

Due to the importance and high impact of emulsions in the petroleum processing steps in the last decades, the application of microfluidic systems for probing the emulsions stability in crude oil mixtures has gained significant attention. In this section, we summarize the key results on the coalescence kinetics of water droplets and stability of crude oil emulsions under different experimental conditions using microfluidic platforms. To enhance the separation of residual water from oil, different additives have been introduced to manipulate the coalescence kinetics of water droplets. For example, Nowbahar et al.[25] examined the effects of six different additives (such as lower and higher molecular weight cellulose ether, polyether-modified siloxane, non-ionic polyether polyol, etc.), where each additive was premixed with the diluted bitumen in naphtha (dilbit) in a T-junction microfluidic setup (see Figure 1a). Here, the authors monitored the performance of each additive in coalescence of emulsion droplets and further estimated the number of coalescence events. As an example, the coalescence of water droplets in diluted bitumen in the presence of 300 ppm lower molecular weight cellulose can be seen in Figure 1b. Here, the coalescence occurred between two or even three water droplets at different frequency rates in different channels. Additionally, in the absence of additive, no coalescence was observed suggesting that the emulsion is possibly stabilized via asphaltenes and/or resins (elastic interface).

To gain deeper insights into the kinetics of coalescence, the number of coalescence events (N_c) can be estimated as follows:

$$N_c = n_0 - n \qquad (1)$$

Here n_0 and n are the number of water droplets at the initial reference point and the number of droplets counted at any given time, respectively.

Figure 1c shows the average number of coalescence events normalized by the initial number of droplets (at t = 0) for different concentrations of additives. At additive concentration of 300 ppm, a proprietary additive (with relative solubility number of 10-13 and kinematic viscosity of ~1000 cSt) resulted in the highest coalescence rate followed by nonionic polyether polyol (see red and orange lines in Figure 1c). The addition of 300 ppm polyether-modified siloxane (light blue) did not induce any droplets coalescence as indicated by N_c= 0.

Furthermore, it was found that the structure of additive can drastically alter the emulsion stability. For example, the two siloxanes including polyether-modified siloxane and hydroxyl-functional polydimethylsiloxane exhibited a very different demulsification property. Unlike the case of polyether-modified siloxane (light blue color) which showed no impact on the emulsion stability, the hydroxyl-functional polydimethylsiloxane (blue color) induced high rate of coalescence between emulsified water droplets. Additionally, the difference in the molecular weight of an additive (e.g., lower and higher molecular weight cellulose ether highlighted in light green and purple lines, respectively) can alter the coalesce frequency and as such the emulsion stability.

There results provide important information on the potential of using various additives with different structures and molecular weights to enhance the coalescence kinetics and the dewatering performance of water-in-crude oil emulsions. Additionally, this calls for an in-depth analysis of interfacial activity of these surface-active agents under different temperature and pressure conditions to optimize the separation efficacy.

As stated in the Introduction, one of the factors involved in the enhancement of water-in-oil emulsion stability is the presence of asphaltene. Asphaltenes have a great tendency toward aggregation and forming a 3-D network at the oil-water interface (rigid interface)[31, 32]. The formation of rigid interface plays a key role in preventing the coalescence of emulsified water droplets. In one of the recent studies conducted by Trabelsi's group, the simultaneous effects of asphaltene and demulsifiers on the stability and coalescence rate of water droplets immersed in two model oils were studied in detail[30]. The authors tested three different demulsifiers, including EO-PO copolymer (EO-PO), alkoxylated polyamine (APA), and polyester polyol (PE) in different surfactants solution and microemulsions. As depicted in Figure 1d, a T-junction microfluidic system was used to probe the formation of water droplets in two asphaltene/heptol mixtures (with different vol (%) ratios of n-heptane and toluene). The coalescence behavior of water emulsions in collision chamber with 500 μm channel width (red magnified region) was monitored, accordingly. To create the emulsions properly, the model oils passed through the microfluidics to fully wet the surfaces with the oil, and then water was injected. To examine the coalescence kinetics of emulsified water droplets, the rate of coalescence can be estimated via the following equations:

$$R_c = \frac{n_c}{A_c\, t_{exp} n_T} \quad (2)$$

$$n_c = \sum_i^j n_{c,ij} \quad (3)$$

R_c and A_c represent the rate of coalescence ($m^{-2}.s^{-1}$) and the monitored contact area (m^2), respectively. t_{exp} is the time of experiment (s), n_T is the total number of initial droplets generated during the experiment, and n_c is the number of coalescence events. Figure 1e shows the gradual evolution of coalescence event for C40 model oil consisting of 2% asphaltene dispersed in 40% heptane and 60% toluene in the presence of EO-PO ME (i.e., 23 wt.% $C_{12-15}E_7$, 23 wt. % isopropyl alcohol, 5 wt.% EO-PO, 34 wt.% Milli-Q water, and 15 wt.% d-limonene) as the aqueous phase. ME stands for microemulsion. Here, coalescence "type 11" represents the coalescence between the two first-generation droplets as they go through the collision chamber (shown in blue dashed line). Coalescence "type 12" is the coalescence between the newly formed droplets from type 11 and another first-generation emulsion droplet. Yellow dashed lines in Figure 1e highlight the formation of larger droplets (referred as type 22) as more coalescence events occur with time. Figure 1f represents the coalescence rate distribution of different coalescence types in C40 model oil including different demulsifiers. As shown in this diagram, EO-PO and APA demulsifiers exhibited wider distribution of coalescence types indicating that these two demulsifiers are more effective in destabilizing the emulsion in comparison with PE. In the case of PE, the coalescence type 11 had the highest distribution rate and no additional coalescence events were recorder which resulted in the lowest coalescence rate. It should be mentioned that the efficiency of demulsifier on the asphaltene-stabilized emulsions is a function of many factors, including crude oil composition, and other physical properties, such as API gravity, temperature, degree of salinity, and aging of emulsions[25].

One of the main limitations of this current apparatus is that it cannot account for the aging effect to systematically probe the evolution of interface in the presence of demulsifier and asphaltenes. Therefore, more attention should be given to the factors involved in altering interfacial properties of W/O interface. In this regard, Fuller's group[33] probed the spontaneous emulsification of water droplet in the hydrocarbon phase containing asphaltenes. In this research, a co-flow microfluidic device was utilized to observe the shrinkage of a water droplet in different asphaltene-hydrocarbons mixtures. The schematic of the co-flow microfluidic is shown in Figure 2a. The initial radius of the emulsion droplet is highlighted with the white line and the change in the droplet size was recorded over time period of 5 hours. As it can be seen in Figure 2a, the droplet size decreases with time while the new micron-sized droplets spontaneously form in the solution. Additionally, the droplet/volume measurements were conducted for different droplet sizes in pure toluene and heptol mixtures (heptane/toluene=40/60) in the absence and presence of asphaltenes. The authors found that in the absence of asphaltenes, the droplet volume almost remained constant during the time of study regardless of oil composition and initial droplet size; see Figure 2b. However, when the solution contained asphaltene, the droplet volume decreased due to the spontaneous emulsification of water droplets (see the results of normalized droplet volume vs. time for different initial droplet sizes in heptol 40/60 in Figure 2c). The trend was more evident, in particular for smaller droplets (e.g., 105 μm vs. 300 μm). Asphaltenes create a viscoelastic/rigid film and result in the spontaneous formation of emulsion droplets. Once pure toluene was used instead of heptane/toluene mixture, the results did not change noticeably suggesting that heptane does not have a major contribution to spontaneous emulsification under the current experimental conditions. The interactions between asphaltene aggregates and the aqueous phase at the interface may be responsible for the spontaneous formation of water droplets. Additionally, it was found that spontaneous emulsification mostly depends on the initial interfacial area and initial inside pressure. Ultimately, to obtain deeper information on the topic, the effects of other oil compositions, such as paraffin, naphthenic acids, and degree of salinity on the interfacial rheology and spontaneous emulsification of water droplets should be examined in the future research studies. Most literature reports that employed microfluidics for water-in-oil emulsion stability analysis have been mainly focused on the effects of different additives/demulsifiers, aging interface, and hydrodynamic forces on the coalescence kinetics of emulsified droplets. Electrocoalescence technology has been used in an industrial level to enhance the coalescence between emulsified water droplets and ultimately separate them from the crude oil and hydrocarbon mixtures[34-37]. Nevertheless, less attention has been paid to the use of electrocoalescence for monitoring the effect of electric field on the crude oil emulsion destabilization in a microporous media[37, 38]. Leary et al.[38] with the aid of microfluidic device generated a two-dimensional (2D) emulsion and further investigated the effect of electrical field on the coalescence of emulsified water droplets.

Figure 2d depicts a flow-focusing microfluidic system used to generate monodispersed water drops in crude oil through orifice that is 50 μm wide. Then, the emulsion droplets were monitored as they pass between the electrodes to see how the applied electric field could affect the stability of emulsion droplets against coalescence. The coalescence study was conducted with the electric field strength of 250 V/mm. As shown in Figures 2e and 2f, no coalescence occurred after 1.94 s, but as time proceeded, the water droplets began to coalesce with each other. The coalescence of water droplets and the formation of larger droplets could be clearly seen at time=2.26 s. Additionally, it was found that the droplets oriented toward the electrical field in the time scale of milliseconds. These results show that the introduction of electric field to the emulsion can potentially affect the asphaltene-asphaltene and/or asphaltene-resin interactions at the interface and as a result weaken the elasticity of emulsion film (this facilitates the coalescence between the water droplets).

Application of microfluidics in crude oil-in-water emulsions (O/W) characterization

Globally, it is estimated that the ratio of produced water to oil during petroleum production is ~3:1. This amount of water should go under further treatment before re-injecting it to the reservoir or discharge in order to remove the dispersed crude oil from water[13]. The offshore produced water system was traditionally used to improve the water treatment quality and it consists of different parts, such as bulk gravity separator, a sand handling system, a hydrocyclone and a gas flotation. Figure 3a shows the schematic diagram of typical water treatment process.

In the previous section, we summarized the literature studies focused on the understanding of the stabilization/destabilization of W/O emulsions. In this section, however, we will investigate the applications of microfluidics in: (i) coalescence kinetics of crude oil droplets emulsified in the aqueous media for water treatment process and (ii) crude oil-brine interface elasticity for enhanced oil recovery.

In this regard, Dudek et al.[13] studied the effect of different parameters including different crude oils, water salinity, pH, dissolved components, and pressure on the coalescence of crude oil droplets. They used custom-designed T-junction glass microfluidic chips with the inlet channels width of 100 μm, coalescence chamber with the width of 500 μm and length of ~33 mm (see Figure 3b for the microfluidic chip setup). All channels had a uniform depth of 45 μm and the oil and water flow rates were set to 10 and 160 μl/min, respectively. Figure 3b shows the coalescence frequencies of six different diluted crude oils in two different brines containing: (i) only NaCl (referred as Na-Brine) and (ii) mixture of NaCl and $CaCl_2$ (referred as NaCa-Brine) at three levels of pH= 4, 6 and 10. The SARA fractions of different crude oils are summarized in Table 1. The results show that the light crude oils (B, D, E, F) show much higher coalescence rates compared with the heavier ones (A and C). Also, an increase in the pH reduced the coalescence frequencies of oil droplets possibly due to the change in the concentration of surface-active components at the interface and altering the component's interfacial activity (see Figures 3c and 3d) [39]. Under the basic conditions, e.g., pH=10, acids (often called naphthenic acids) exhibit higher interfacial activity and therefore they can enhance the stability of oil droplets against coalescence. It is worth mentioning that increasing pH also accelerates the deprotonation of more acidic species resulting in increased interfacial concentration and enhanced emulsion stability[40]. Additionally, different brine solutions exhibit different interfacial activity. For example, the addition of divalent ions (calcium) to the solution can result in the formation of acid-calcium complexes, eliminate acidic species from the interface and reduce the interfacial activity. This phenomenon enhances the diffusion rate of acids from the interface to the oil phase and possibly leading to the increase rate of droplets coalescence[41]. This trend is more evident at pH=10. Figure 3e shows the coalescence frequencies vs. the sum of resin and asphaltene weight fractions of the crude oils. The results revealed that the coalescence frequencies drop exponentially with an increase in the total resin and asphaltene weight fractions. Resins are interfacially active molecules which can affect the coalescence of oil droplets by enhancing the electrostatic repulsion between the droplets. However, the repulsion forces are suppressed noticeably due to the high concentration of electrolyte in the solution. As already stated, asphaltenes play a key role in the stability of crude oil emulsions through the formation of 3D network at the interface. An increase in the asphaltene content, enhances the elastic properties of O/W interface (rigid interface) and this can reduce the coalescence frequencies of oil droplets to a great extent.

In the later study, the authors extended their methodology to ten different crude oils, more complex water compositions and further examined the effect of droplet aging[42]. Additionally, they investigated the effect of different chip design (e.g., variable channel length and coalescence chamber dimensions) on coalescence frequency of oil droplets. There are various experimental factors that directly affect the interfacial activity of resins, asphaltenes, and naphthenic acids, including water pH, salinity, and ionic composition of the brine. The different properties O/W interface such as strength and elasticity of the interfacial layers were known to be determined by the type of interfacially active components. Their results showed that addition of the dissolved components to the water phase can alter the droplet-droplet coalescence kinetics in most of the crude oils. Additionally, they observed that using synthetic produced water (SPW; containing Na^{+}, Ca^{2+}, and Mg^{2+} cations and Cl^{-}, HCO^{3-}, and $SO4^{2-}$ anions) cause reduction or induce no change in the coalescence of oil droplets. This trend could be due to the precipitation of carbonate salts and their adsorption at the O/W interface, which could affect the emulsion stability via Pickering stabilization[43].

The effect of aging on coalescence was investigated based on different channel length. The oil droplets coalescence frequency was significantly lower in long channels vs. both medium and short channels even under different experimental conditions including different pH, acids, and salt composition of water phase (see Figure 3f). Formation of new droplets from the bulk oil phase results in the creation of new interface which is a location for the diffusion of interfacially active components. Their adsorption at the O/W interface decrease the interfacial tension and form viscoelastic interfacial layers which can potentially affect the coalescence probability of oil droplets[44, 45]. It was shown that aging of the interface could in fact decrease the coalescence probability of crude oil droplets noticeably. The adsorption of asphaltenes and their rearrangement at the aged interface enhances the interface elasticity and resistance against coalescence[45, 46].

They also investigate the effect of channel size on droplet size as well as the coalescence frequency. The observed that every crude oil exhibit distinct behavior, however, most crude oils show reduction in the coalescence frequency as a result of the increase in size of the droplets in different position inside the channel.

Microfluidic platforms to probe the interfacial elasticity of crude oil-brine

Microfluidic platforms allow for the direct observation of multiphase displacements inside a porous media and under flow conditions. These miniaturized systems can be used to mimic the flow dynamics occurring at the pore-scale by generating droplets in a manner resembling snap-off events occurring in pores and pore-throat junctions in the natural reservoir rocks. Once oil flows through a water-wet constriction area into a pore filled with water, the interfacial forces could cause oil phase to separate into a droplet (snap off) and become trapped within a pore[47]. Snap-off process is affected by the chemistry of aqueous phase and is shown to play an important role in the crude oil recovery. To mimic this phenomenon inside a porous media, Morin et al.[48] used a flow-focusing microfluidic platform to generate oil droplets via extensional flows to understand how snap-off is influenced by interfacial properties (e.g., viscoelasticity) evolved under static conditions during aging of oil inside pores.

Figures 4a and 4b represent the schematic of snap-off event in a porous media and a flow-focusing microfluidic chip to examine the effects of interfacial elasticity on the snap-off. Figure 4c shows the differences in the dynamics of snap-off evolution as the crude oil aged against low salinity brine (1%) and high salinity brine (100%). In low salinity brine, the results highlight that the crude oil forms a long thread and extends over the channel junction. In this case, the formation of viscoelastic interface plays a key role in the flow stability and suppressing the snap-off. Additionally, numerical analysis of the critical shear force needed for snap-off for two different crude oils; Timber Creek (TC) and Gibbs Field (GF) sourced from Wyoming, aged in both low and high salinity brine was performed using finite element computational fluid dynamics. Figure 4d shows that in low salinity brine the shear force increased during the process of snap-off indicating an enhancement in the interface viscoelasticity due to the presence of asphaltenes and other interfacially active components in crude oil (considering interfacial tension of crude oil and brine did not change with salinity). However, in high salinity brine, the normalized shear force driving snap-off remains constant during the time of simulation; see Figure 4e. This further indicates that the force was enough to cause snap-off and no viscoelastic resistance was observed during the elongation of crude oil. Additionally, Liu et al.[49]. investigated the effects of asphaltene content, composition and concentration of brine and crude oil on the interface elasticity of crude oil-brine. Figure 4f shows that in the high salinity brine (100% salinity, 666.94 mmolal NaCl) the average droplet size does not change even once the asphaltene concentration increases from 0 to 5%. However, in low salinity condition (1% salinity, 0.67 mmolal NaCl), the droplet size increases significantly with increase in the asphaltene content. This further indicate that increasing the asphaltene content augments the suppression of snap-off under low salinity condition through altering the interfacial elasticity of crude oil-brine. It should be mentioned that in high salinity brine, it is likely that no elastic film (or weak film) was formed and only the interfacial tension and viscous forces contributed to the snap-off process. Additionally, the authors investigated the effect of aging the interface on the oil droplet size using different brine solutions. Figure 4g shows that under high salinity conditions, aging the interface does not prevent the snap-off (except the case of KCl). Under low salinity conditions, however, different trend was observed with aging the interface. For example, in the presence of KCl and $CaCl_2$ brines, aging had no significant effect on altering the interfacial elasticity and droplet size. Nevertheless, in the presence of NaCl, the droplet size increased significantly with aging. Interestingly, in the case of $MgCl_2$ the droplet breakup occurred faster after aging suggesting the formation of less elastic interface. Overall, under low salinity conditions, aging allows asphaltene molecules to adsorb and rearrange at the interface resulting in the enhancement of interfacial elasticity[50, 51]. However, based on the results obtained in the case of $MgCl_2$, it can be inferred that that adsorption of asphaltene molecules and their interactions at the interface is reversible and aging could even weaken the elasticity of interface.

The electrostatic interactions between the cations in brine and surface-active agents as well as other species (e.g., resins and asphaltenes) in crude oil can govern the interfacial properties of crude oil and brine. Additionally, the acids present in crude oil can diffuse into the aqueous phase, dissociate, and form a complex with metal cations. As a result, the interfacial properties could be also altered by adsorption of acids at the interface. The competition between acids and asphaltene molecules at the interface could drastically affect the interfacial elasticity of crude oil-brine. For example, under high salinity conditions, high concentration of cations promotes the adsorption of acids which can interfere with the asphaltene-asphaltene interactions at the interface and prevent the formation of elastic film (see the schematic of proposed mechanism in Figure 4h). However, under low salinity conditions, less acids are present at the interface and this allows asphaltene molecules to interact strongly and enhance the interfacial elasticity[52].

Concluding Remarks

While microfluidic systems with various designs have been extensively employed in crude/heavy oil related studies, the full utilization of the benefits that microfluidics brings and more wide acceptance in the industrial applications is still in its initial stages. Some important advantages of lab-on-chip devices are the option of using small samples and performing fast measurements. Microfluidic platforms can closely mimic the pores and pore throats observed in the natural rocks and further allows for the direct visualization of fluid flow, multiphase displacements, and emulsion formation at the length scales comparable to the reservoir pore sizes. Microfluidic platforms are potential tools to investigate the stability of water-in-crude oil (W/O) and crude oil-in-water (O/W) emulsions. Furthermore, specific confined geometries in microfluidic devices cultivates a proper route for measurement of interfacial tension (IFT[53]) and spontaneous emulsification[33] phenomena in crude emulsion systems at the short time scales.

The interactions between different crude oil species including asphaltene-asphaltene and asphaltene-resin are shown to enhance the stability of crude oil emulsions as they encourage the formation of rigid interface. Demulsifiers can facilitate the coalescence of water droplets in crude oil by adsorbing at the interface and weakening the elasticity of interfacial film. However, superiority of one additive over another is likely related to its chemical structure and interfacial activity, which is yet to be understood. The introduction of demulsifiers to the crude oil systems either before or after the formation of water droplets in a microchannel alters the coalescence rate and the emulsion stability. The aging of emulsion and the different time scales for adsorption of asphaltenes (and other fractions of crude oil) and demulsifiers at the interface can explain these variations observed in the coalescence kinetics. Nevertheless, the presence of salts and acids can drastically affect the interfacial properties of water/oil interface and therefore should be studied along with the presence of demulsifiers. Methodologies that can provide robust measurements of interfacial rheology (such as interfacial tension and elastic properties) under different conditions, including different water pH and solvent to bitumen ratio are yet missing in the literature reports. It should be mentioned that the induced shear in microfluidic devices can alter the water/oil interfacial properties. High shears can affect the arrangement and accumulation of asphaltene aggregates as well as other fine particles at the interface, and subsequently alter the coalescence of emulsified droplets. Therefore, more attention should be given to fairly compare the interfacial properties of water/oil measured at the microscale vs. bulk.

Understanding the mechanisms and kinetics of coalescence between crude oil droplets in water (O/W) in confinement geometry are crucial in water treatment process. Extensive efforts should be undertaken to evaluate the effects of asphaltenes and acids content, emulsion aging, and metal cations on the emulsion stability. Additionally, different types of additives/demulsifiers can be added to the emulsions to identify the proper combinations of additives and time scale required to facilitate the droplet-droplet coalescence. In crude oil emulsion studies via microfluidic chips, the application of robust numerical methods (e.g., population balance modeling[54, 55] and artificial intelligence[56]) to model the growth of droplets due to the coalescence in the presence of surface-active species[57] and solid particles have not been explored in detail.

The porous media in natural rocks has heterogenous surface and is composed of minerals, such as diatomite and calcite making it different than conventional lab-on-a-chip systems. However, very limited studies have investigated the use of natural rocks and/or surface treatment (i.e., $CaCO_3$ growth) to probe the properties of multiphase flows in a confined geometry[58-63]. These natural rock micromodels can be used to study the formation of crude oil emulsions and the interfacial properties of water/oil under various experimental conditions, including different solvent/bitumen ratio, salinity, temperature, and pH.

Author Information

Corresponding Authors

nn1@ualberta.ca; saeedm6@vt.edu

Notes

The authors declare no conflict of interest.

Acknowledgments

We greatly thank Dr. Plamen Tchoukov and Dr. Jan Czarnecki at the University of Alberta for their productive feedback on the formation and stability of crude oil emulsions.

References

1. Whitesides, G. M., The origins and the future of microfluidics. *nature* **2006,** *442* (7101), 368-373.
2. Niculescu, A.-G.; Chircov, C.; Bîrcă, A. C.; Grumezescu, A. M., Fabrication and Applications of Microfluidic Devices: A Review. *International Journal of Molecular Sciences* **2021,** *22* (4), 2011.
3. Mozaffari, S.; Ghasemi, H.; Tchoukov, P.; Czarnecki, J.; Nazemifard, N., Lab-on-a-Chip Systems in Asphaltene Characterization: A Review of Recent Advances. *Energy & Fuels* **2021**.
4. Pan, L.-J.; Tu, J.-W.; Ma, H.-T.; Yang, Y.-J.; Tian, Z.-Q.; Pang, D.-W.; Zhang, Z.-L., Controllable synthesis of nanocrystals in droplet reactors. *Lab on a Chip* **2018,** *18* (1), 41-56.
5. Wongkaew, N.; Simsek, M.; Griesche, C.; Baeumner, A. J., Functional nanomaterials and nanostructures enhancing electrochemical biosensors and lab-on-a-chip performances: recent progress, applications, and future perspective. *Chemical reviews* **2018,** *119* (1), 120-194.
6. Gerhardt, R. F.; Peretzki, A. J.; Piendl, S. K.; Belder, D., Seamless combination of high-pressure chip-HPLC and droplet microfluidics on an integrated microfluidic glass chip. *Analytical chemistry* **2017,** *89* (23), 13030-13037.
7. Wlodarczyk, K. L.; Hand, D. P.; Maroto-Valer, M. M., Maskless, rapid manufacturing of glass microfluidic devices using a picosecond pulsed laser. *Scientific reports* **2019,** *9* (1), 1-13.
8. Oyama, T. G.; Oyama, K.; Taguchi, M., A simple method for production of hydrophilic, rigid, and sterilized multi-layer 3D integrated polydimethylsiloxane microfluidic chips. *Lab on a Chip* **2020,** *20* (13), 2354-2363.
9. Bazazi, P.; Sanati-Nezhad, A.; Hejazi, S. H., Role of chemical additives on water-based heavy oil mobilization: A microfluidic approach. *Fuel* **2019,** *241*, 1195-1202.
10. Bao, B.; Riordon, J.; Mostowfi, F.; Sinton, D., Microfluidic and nanofluidic phase behaviour characterization for industrial CO 2, oil and gas. *Lab on a Chip* **2017,** *17* (16), 2740-2759.
11. Luo, J.; Dziubla, T.; Eitel, R., A low temperature co-fired ceramic based microfluidic Clark-type oxygen sensor for real-time oxygen sensing. *Sensors and Actuators B: Chemical* **2017,** *240*, 392-397.
12. Mazutis, L.; Griffiths, A. D., Selective droplet coalescence using microfluidic systems. *Lab on a Chip* **2012,** *12* (10), 1800-1806.
13. Dudek, M.; Bertheussen, A.; Dumaire, T.; Øye, G., Microfluidic tools for studying coalescence of crude oil droplets in produced water. *Chemical Engineering Science* **2018,** *191*, 448-458.
14. Mozaffari, S.; Tchoukov, P.; Mozaffari, A.; Atias, J.; Czarnecki, J.; Nazemifard, N., Capillary driven flow in nanochannels–Application to heavy oil rheology studies. *Colloids and Surfaces A: Physicochemical and Engineering Aspects* **2017,** *513*, 178-187.
15. Mozaffari, S.; Tchoukov, P.; Atias, J.; Czarnecki, J.; Nazemifard, N., Effect of Asphaltene Aggregation on Rheological Properties of Diluted Athabasca Bitumen. *Energy & Fuels* **2015,** *29* (9), 5595-5599.
16. Langevin, D.; Poteau, S.; Hénaut, I.; Argillier, J., Crude oil emulsion properties and their application to heavy oil transportation. *Oil & gas science and technology* **2004,** *59* (5), 511-521.
17. Alboudwarej, H.; Muhammad, M.; Shahraki, A. K.; Dubey, S.; Vreenegoor, L.; Saleh, J. M., Rheology of heavy-oil emulsions. *SPE Production & Operations* **2007,** *22* (03), 285-293.
18. Kolotova, D. S.; Kuchina, Y. A.; Petrova, L. A.; Voron'ko, N. G.; Derkach, S. R., Rheology of water-in-crude oil emulsions: Influence of concentration and temperature. *Colloids and Interfaces* **2018,** *2* (4), 64.
19. Rane, J. P.; Pauchard, V.; Couzis, A.; Banerjee, S., Interfacial rheology of asphaltenes at oil–water interfaces and interpretation of the equation of state. *Langmuir* **2013,** *29* (15), 4750-4759.

20. Rezaee, S.; Tavakkoli, M.; Doherty, R.; Vargas, F. M., A new experimental method for a fast and reliable quantification of saturates, aromatics, resins, and asphaltenes in crude oils. *Petroleum Science and Technology* **2020,** *38* (21), 955-961.
21. Enayat, S.; Babu, N. R.; Kuang, J.; Rezaee, S.; Lu, H.; Tavakkoli, M.; Wang, J.; Vargas, F. M., On the development of experimental methods to determine the rates of asphaltene precipitation, aggregation, and deposition. *Fuel* **2020,** *260*, 116250.
22. Saad, M.; Kamil, M.; Abdurahman, N.; Yunus, R. M.; Awad, O. I., An overview of recent advances in state-of-the-art techniques in the demulsification of crude oil emulsions. *Processes* **2019,** *7* (7), 470.
23. da Silva, M.; Sad, C. M.; Pereira, L. B.; Corona, R. R.; Bassane, J. F.; dos Santos, F. D.; Neto, D. M.; Silva, S. R.; Castro, E. V.; Filgueiras, P. R., Study of the stability and homogeneity of water in oil emulsions of heavy oil. *Fuel* **2018,** *226*, 278-285.
24. Mozaffari, S., Rheology of Bitumen at the Onset of Asphaltene Aggregation and its Effects on the Stability of Water-in-Oil Emulsion. **2015**.
25. Nowbahar, A.; Whitaker, K. A.; Schmitt, A. K.; Kuo, T.-C., Mechanistic study of water droplet coalescence and flocculation in diluted bitumen emulsions with additives using microfluidics. *Energy & Fuels* **2017,** *31* (10), 10555-10565.
26. Chesters, A. K., Modelling of coalescence processes in fluid-liquid dispersions: a review of current understanding. *Chemical engineering research and design* **1991,** *69* (A4), 259-270.
27. Hong, Z.; Jianhua, X.; Zhenggui, S.; Jian, Z.; Yongming, Z.; Fanghui, W., Application of nanometer-silicon dioxide in tertiary oil recovery. *Acta Petrolei Sinica* **2006,** *27* (6), 96.
28. Khaleduzzaman, S.; Mahbubul, I.; Shahrul, I.; Saidur, R., Effect of particle concentration, temperature and surfactant on surface tension of nanofluids. *International Communications in Heat and Mass Transfer* **2013,** *49*, 110-114.
29. Goel, S.; Ng, S.; Acosta, E.; Ramachandran, A., The roles of contact time and contact pressure on the coalescence of water droplets suspended in concentrated bitumen solutions. *Fuel* **2018,** *223*, 486-495.
30. Lin, Y.-J.; Perrard, A.; Biswal, S. L.; Hill, R. M.; Trabelsi, S., Microfluidic investigation of asphaltenes-stabilized water-in-oil emulsions. *Energy & Fuels* **2018,** *32* (4), 4903-4910.
31. Czarnecki, J.; Tchoukov, P.; Dabros, T., Possible role of asphaltenes in the stabilization of water-in-crude oil emulsions. *Energy & Fuels* **2012,** *26* (9), 5782-5786.
32. Tchoukov, P.; Yang, F.; Xu, Z.; Dabros, T.; Czarnecki, J.; Sjoblom, J., Role of asphaltenes in stabilizing thin liquid emulsion films. *Langmuir* **2014,** *30* (11), 3024-3033.
33. de Araujo, S. B.; Reyssat, M.; Monteux, C.; Fuller, G., Ablation of water drops suspended in asphaltene/heptol solutions due to spontaneous emulsification. *Science advances* **2019,** *5* (10), eaax8227.
34. Eow, J. S.; Ghadiri, M., Electrostatic enhancement of coalescence of water droplets in oil: a review of the technology. *Chemical Engineering Journal* **2002,** *85* (2-3), 357-368.
35. Perles, C. E.; Volpe, P. L. O. f.; Bombard, A. n. J., Study of the cation and salinity effect on electrocoalescence of water/crude oil emulsions. *Energy & fuels* **2012,** *26* (11), 6914-6924.
36. Less, S.; Hannisdal, A.; Sjöblom, J., An electrorheological study on the behavior of water-in-crude oil emulsions under influence of a DC electric field and different flow conditions. *Journal of dispersion science and technology* **2008,** *29* (1), 106-114.
37. Mostowfi, F.; Czarnecki, J.; Masliyah, J.; Bhattacharjee, S., A microfluidic electrochemical detection technique for assessing stability of thin films and emulsions. *Journal of colloid and interface science* **2008,** *317* (2), 593-603.
38. Leary, T.; Yeganeh, M.; Maldarelli, C., Microfluidic study of the electrocoalescence of aqueous droplets in crude oil. *ACS omega* **2020,** *5* (13), 7348-7360.
39. Arla, D.; Sinquin, A.; Palermo, T.; Hurtevent, C.; Graciaa, A.; Dicharry, C., Influence of pH and water content on the type and stability of acidic crude oil emulsions. *Energy & fuels* **2007,** *21* (3), 1337-1342.

40. Havre, T. E.; Sjöblom, J.; Vindstad, J. E., Oil/water-partitioning and interfacial behavior of naphthenic acids. *Journal of dispersion science and technology* **2003,** *24* (6), 789-801.

41. Tichelkamp, T.; Teigen, E.; Nourani, M.; Øye, G., Systematic study of the effect of electrolyte composition on interfacial tensions between surfactant solutions and crude oils. *Chemical Engineering Science* **2015,** *132*, 244-249.

42. Dudek, M.; Chicault, J.; Øye, G., Microfluidic Investigation of Crude Oil Droplet Coalescence: Effect of Oil/Water Composition and Droplet Aging. *Energy & Fuels* **2019,** *34* (5), 5110-5120.

43. Binks, B. P.; Rodrigues, J. A.; Frith, W. J., Synergistic interaction in emulsions stabilized by a mixture of silica nanoparticles and cationic surfactant. *Langmuir* **2007,** *23* (7), 3626-3636.

44. Arla, D.; Flesisnki, L.; Bouriat, P.; Dicharry, C., Influence of alkaline pH on the rheology of water/acidic crude oil interface. *Energy & Fuels* **2011,** *25* (3), 1118-1126.

45. Moran, K.; Sumner, R., Aging effects on surface properties and coalescence of bitumen droplets. *The Canadian Journal of Chemical Engineering* **2007,** *85* (5), 643-653.

46. Harbottle, D.; Chen, Q.; Moorthy, K.; Wang, L.; Xu, S.; Liu, Q.; Sjoblom, J.; Xu, Z., Problematic stabilizing films in petroleum emulsions: Shear rheological response of viscoelastic asphaltene films and the effect on drop coalescence. *Langmuir* **2014,** *30* (23), 6730-6738.

47. Roof, J., Snap-off of oil droplets in water-wet pores. *Society of Petroleum Engineers Journal* **1970,** *10* (01), 85-90.

48. Morin, B.; Liu, Y.; Alvarado, V.; Oakey, J., A microfluidic flow focusing platform to screen the evolution of crude oil–brine interfacial elasticity. *Lab on a Chip* **2016,** *16* (16), 3074-3081.

49. Liu, Y.; Kaszuba, J.; Oakey, J., Microfluidic investigations of crude oil-brine interface elasticity modifications via brine chemistry to enhance oil recovery. *Fuel* **2019,** *239*, 338-346.

50. Verruto, V. J.; Le, R. K.; Kilpatrick, P. K., Adsorption and molecular rearrangement of amphoteric species at oil– water interfaces. *The Journal of Physical Chemistry B* **2009,** *113* (42), 13788-13799.

51. Kilpatrick, P. K., Water-in-Crude Oil Emulsion Stabilization: Review and Unanswered Questions. *Energy & Fuels* **2012,** *26* (7), 4017-4026.

52. Chávez-Miyauchi, T. s. E.; Firoozabadi, A.; Fuller, G. G., Nonmonotonic elasticity of the crude oil–brine interface in relation to improved oil recovery. *Langmuir* **2016,** *32* (9), 2192-2198.

53. Goel, S.; Joshi, N.; Uddin, M. S.; Ng, S.; Acosta, E.; Ramachandran, A., Interfacial Tension of the Water-Diluted Bitumen Interface at High Bitumen Concentrations Measured Using a Microfluidic Technique. *Langmuir* **2019,** *35* (48), 15710-15722.

54. Zhao, Z.; Xi, Z.; Jia, N.; Yang, D., A Population Balance Model for Emulsion Behavior of Alkaline Water–Heavy Oil Systems in Bulk Phase. *Energy & Fuels* **2021**.

55. Mozaffari, S.; Li, W.; Dixit, M.; Seifert, S.; Lee, B.; Kovarik, L.; Mpourmpakis, G.; Karim, A. M., The role of nanoparticle size and ligand coverage in size focusing of colloidal metal nanoparticles. *Nanoscale Advances* **2019,** *1* (10), 4052-4066.

56. Adewunmi, A. A.; Kamal, M. S.; Olatunji, S. O., Demulsification of crude oil emulsions using ionic liquids: A computational intelligence approach. *Journal of Petroleum Science and Engineering* **2021**, 109279.

57. Ghasemi, H.; Darjani, S.; Mazloomi, H.; Mozaffari, S., Preparation of stable multiple emulsions using food-grade emulsifiers: evaluating the effects of emulsifier concentration, W/O phase ratio, and emulsification process. *SN Applied Sciences* **2020,** *2* (12), 1-9.

58. Song, W.; de Haas, T. W.; Fadaei, H.; Sinton, D., Chip-off-the-old-rock: the study of reservoir-relevant geological processes with real-rock micromodels. *Lab on a Chip* **2014,** *14* (22), 4382-4390.

59. Porter, M. L.; Jiménez-Martínez, J.; Martinez, R.; McCulloch, Q.; Carey, J. W.; Viswanathan, H. S., Geo-material microfluidics at reservoir conditions for subsurface energy resource applications. *Lab on a Chip* **2015,** *15* (20), 4044-4053.

60. Bowden, S. A.; Tanino, Y.; Akamairo, B.; Christensen, M., Recreating mineralogical petrographic heterogeneity within microfluidic chips: assembly, examples, and applications. *Lab on a Chip* **2016,** *16* (24), 4677-4681.
61. Zhang, Y.; Yesiloz, G.; Sharahi, H. J.; Khorshidian, H.; Kim, S.; Sanati-Nezhad, A.; Hejazi, S. H., Geomaterial-functionalized microfluidic devices using a universal surface modification approach. *Advanced Materials Interfaces* **2019,** *6* (23), 1900995.
62. Yun, W.; Chang, S.; Cogswell, D. A.; Eichmann, S. L.; Gizzatov, A.; Thomas, G.; Al-Hazza, N.; Abdel-Fattah, A.; Wang, W., Toward reservoir-on-a-chip: rapid performance evaluation of enhanced oil recovery surfactants for carbonate reservoirs using a calcite-coated micromodel. *Scientific reports* **2020,** *10* (1), 1-12.
63. Wang, W.; Chang, S.; Gizzatov, A., Toward reservoir-on-a-chip: fabricating reservoir micromodels by in situ growing calcium carbonate nanocrystals in microfluidic channels. *ACS applied materials & interfaces* **2017,** *9* (34), 29380-29386.

Table 1. Saturate, aromatic, resin, and asphaltene (SARA) fractions of different crude oils (A-F). Table reprinted with permission from ref[13]. Copyright 2018 Elsevier.

Crude Oil	SARA [%wt]			
	Saturates	Aromatics	Resins	Asphaltenes
A	50.6	31.2	15.7	2.5
B	84.0	13.4	2.3	0.3
C	64.9	26.3	8.4	0.4
D	71.5	23.1	5.1	0.3
E	74.8	23.2	1.9	0.1
F	78.5	18.9	2.5	0.1

Figure 1. a) Schematic of droplet formation with additive premixed in the diluted bitumen solution using a T-junction microfluidic platform. The widths of constriction and serpentine channels are 50 μm and 1000 μm, respectively. (b) Bright-field microscopy image of emulsion droplets and their coalescence while using 300 ppm low molecular weight cellulose ether (additive) at t = 268 s. (c) Evolution of number of coalescence events (N_c) which is normalized by the initial number of emulsion droplets (n_0) for different additives: 300 ppm proprietary additive (red), lower molecular weight cellulose ether with different concentrations of 1000 ppm (dark green), 300 ppm (light green), and 75 ppm (lightest green). 300 ppm higher molecular weight cellulose ether (purple), 300 ppm nonionic polyether polyol (orange), 300 ppm polyether-modified, hydroxyl-functional polydimethylsiloxane (blue), 300 ppm polyether-modified siloxane (light blue), and control in the absence of any additive (black dashed line). Brown × represents a repeat experiment for the case of nonionic polyether polyol (orange) to confirm reproducibility. Panels a-c reprinted with permission from ref[25]. Copyright 2017 American Chemical Society. (d) Schematic of microfluidic chip setup and the corresponding droplet formation. The width and the height of channel are 100 μm and 50 μm, respectively. The width of collision chamber is 500 μm. (e) Time evolution of coalescence events between emulsion droplets as they go through the chamber using C40 model oil and the aqueous phase containing 0.2% (5 wt. % EO-PO ME). (f) Coalescence rate distribution of different coalescence types in C40 model oil using different demulsifiers: (i) 5 wt. % EO-PO ME, (ii) 5 wt. % APA ME, and (iii) 5 wt. % PE ME. ME stands for microemulsion. The inset plot represents the coalescence rate for each demulsifier. Panels d-f reprinted with permission from ref[30]. Copyright 2018 American Chemical Society.

Figure 2. (a) Schematic diagram of co-flow microfluidic platform. The initial radius of droplet is shown with the white line and the change in the droplet size was recorded during the time of 5 hours. The concentration of asphaltenes in toluene is 1 mg/ml. Normalized water droplet volume versus time while accounting for droplets with various initial sizes: (b) the oil phase consists of heptane/toluene (40/60 vol%) and (c) 1 mg/ml asphaltenes were dispersed in a heptane/toluene (40/60 vol%). Panels a-c reprinted with permission from ref [33]. Copyright 2019 American Association for the Advancement of Science. (d) Schematic of flow focusing microfluidic to generate 2D emulsion droplets in the presence of applied electric field. The width and height of chamber are 3000 μm and 60 μm, respectively. (e,f) Microscopy images of droplets coalescence in at different time intervals (1.94 s and 2.26 s). The scale bar=50 μm. The electric field is employed from top to bottom at $\varepsilon_{electrode}$= 250 V/mm. Panels d-f reprinted with permission from ref [38]. Copyright 2020 American Chemical Society.

Figure 3. (a) Schematic of produced water treatment process, (b) Schematic of microfluidic setup for emulsion generation, (c) Coalescence frequencies of diluted crude oils in Na-Brine (only NaCl) and (d) NaCa-Brine (a mixture of NaCl and $CaCl_2$) at three different pH values, (e) Coalescence frequencies of diluted crude oils as a function of the sum of resins and asphaltenes for different crude oils. The widths of inlet channels and coalescence chamber are 100 μm and 500 μm, respectively. The depth of all channels is 45 μm. Panels a-e reprinted with permission from ref[13]. Copyright 2018 Elsevier. (f) Coalescence frequencies of crude oil droplets under different experimental conditions as a function of aging time. Panel f reprinted with permission from ref[42]. Copyright 2019 American Chemical Society.

Figure 4. (a) Schematic of snap-off in a porous media; (b) Photograph of flow-focusing microfluidic chip to examine the evolution of interfacial elasticity and their effect on the snap-off. The dark liquid represents the oil phase which is aged against transparent brine; (c) Drop formation and evolution of snap-off for crude oil against both low and high salinity brines. The height of rectangular channel is 20 μm. (d) Normalized shear force during snap-off process obtained via computational fluid dynamics for two different crude oils sourced aged vs. low salinity brine (e) and high salinity brine. Panels a-e reprinted with permission from ref[48]. Copyright 2016 Royal Society of Chemistry. (f) Droplet size as a function of asphaltene content for different oils aged against NaCl brine under low and high salinity conditions (100% salinity=666.94 mmolal, 1% salinity=6.67 mmolal); (g) Droplet size vs. different brine compositions under: (i) non-aging (light bars) and (ii) aging (solid bars) conditions ("HS" and "LS" represent low and high salinity, respectively); and (h) Schematic of the proposed mechanism showing the competition between acids and asphaltene molecules and their possible effects on the interfacial properties under low and high salinity conditions for both non-aging and aging interfaces. Possible acid dissociation and complexation with metal cations are depicted in the solid box. "~" is the asphaltene molecules and "acid" shaded with green demonstrates complexation with metal cations. The bold dashed line in black is representative of interface with enhanced elasticity. Panels f-h reprinted with permission from ref[49]. Copyright 2019 Elsevier.

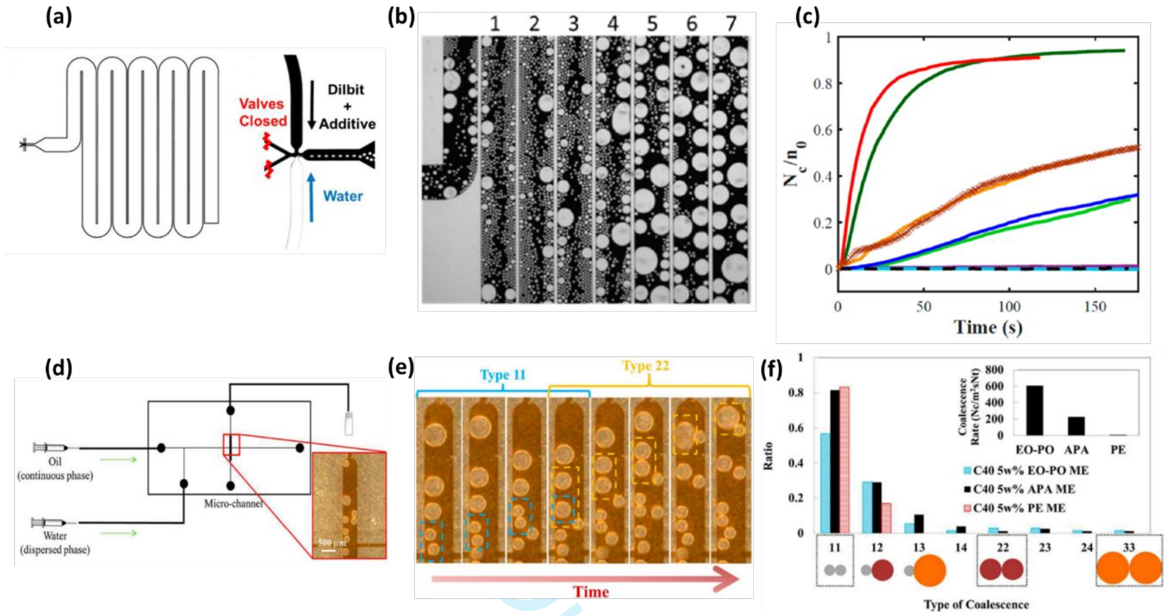

Figure 1. a) Schematic of droplet formation with additive premixed in the diluted bitumen solution using a T-junction microfluidic platform. The widths of constriction and serpentine channels are 50 µm and 1000 µm, respectively. (b) Bright-field microscopy image of emulsion droplets and their coalescence while using 300 ppm low molecular weight cellulose ether (additive) at t = 268 s. (c) Evolution of number of coalescence events (N_c) which is normalized by the initial number of emulsion droplets (n_0) for different additives: 300 ppm proprietary additive (red), lower molecular weight cellulose ether with different concentrations of 1000 ppm (dark green), 300 ppm (light green), and 75 ppm (lightest green). 300 ppm higher molecular weight cellulose ether (purple), 300 ppm nonionic polyether polyol (orange), 300 ppm polyether-modified, hydroxyl-functional polydimethylsiloxane (blue), 300 ppm polyether-modified siloxane (light blue), and control in the absence of any additive (black dashed line). Brown × represents a repeat experiment for the case of nonionic polyether polyol (orange) to confirm reproducibility. Panels a-c reprinted with permission from ref[25]. Copyright 2017 American Chemical Society. (d) Schematic of microfluidic chip setup and the corresponding droplet formation. The width and the height of channel are 100 µm and 50 µm, respectively. The width of collision chamber is 500 µm. (e) Time evolution of coalescence events between emulsion droplets as they go through the chamber using C40 model oil and the aqueous phase containing 0.2% (5 wt. % EO-PO ME). (f) Coalescence rate distribution of different coalescence types in C40 model oil using different demulsifiers: (i) 5 wt. % EO-PO ME, (ii) 5 wt. % APA ME, and (iii) 5 wt. % PE ME. ME stands for microemulsion. The inset plot represents the coalescence rate for each demulsifier. Panels d-f reprinted with permission from ref[30]. Copyright 2018 American Chemical Society.

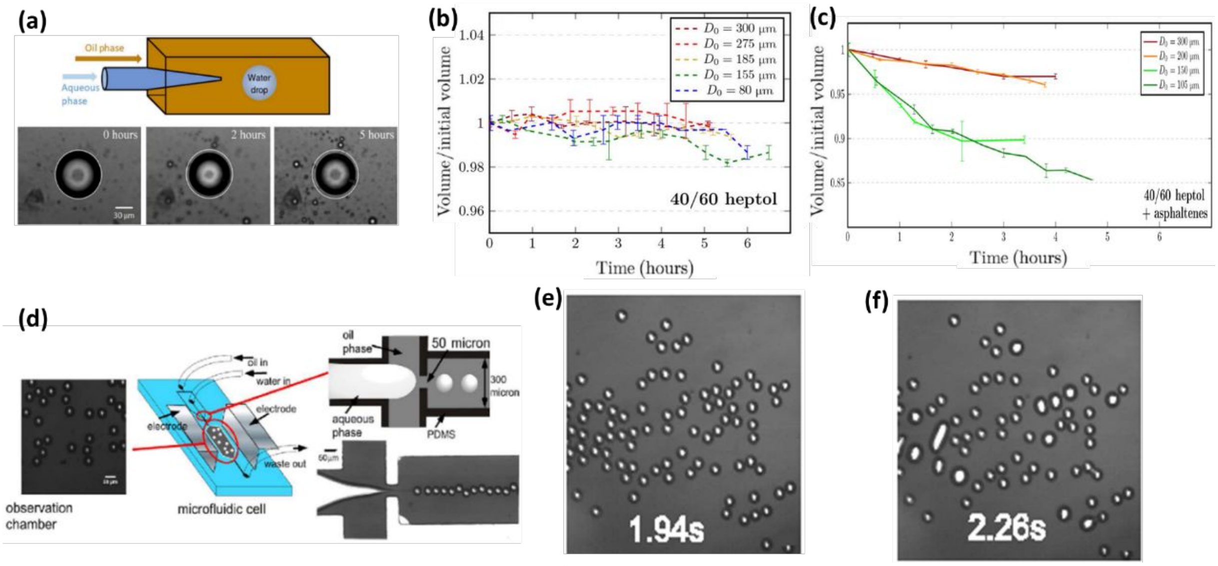

Figure 2. (a) Schematic diagram of co-flow microfluidic platform. The initial radius of droplet is shown with the white line and the change in the droplet size was recorded during the time of 5 hours. The concentration of asphaltenes in toluene is 1 mg/ml. Normalized water droplet volume versus time while accounting for droplets with various initial sizes: (b) the oil phase consists of heptane/toluene (40/60 vol%) and (c) 1 mg/ml asphaltenes were dispersed in a heptane/toluene (40/60 vol%). Panels a-c reprinted with permission from ref [33]. Copyright 2019 American Association for the Advancement of Science. (d) Schematic of flow focusing microfluidic to generate 2D emulsion droplets in the presence of applied electric field. The width and height of chamber are 3000 μm and 60 μm, respectively. (e,f) Microscopy images of droplets coalescence in at different time intervals (1.94 s and 2.26 s). The scale bar=50 μm. The electric field is employed from top to bottom at $\varepsilon_{electrode}$= 250 V/mm. Panels d-f reprinted with permission from ref [38]. Copyright 2020 American Chemical Society.

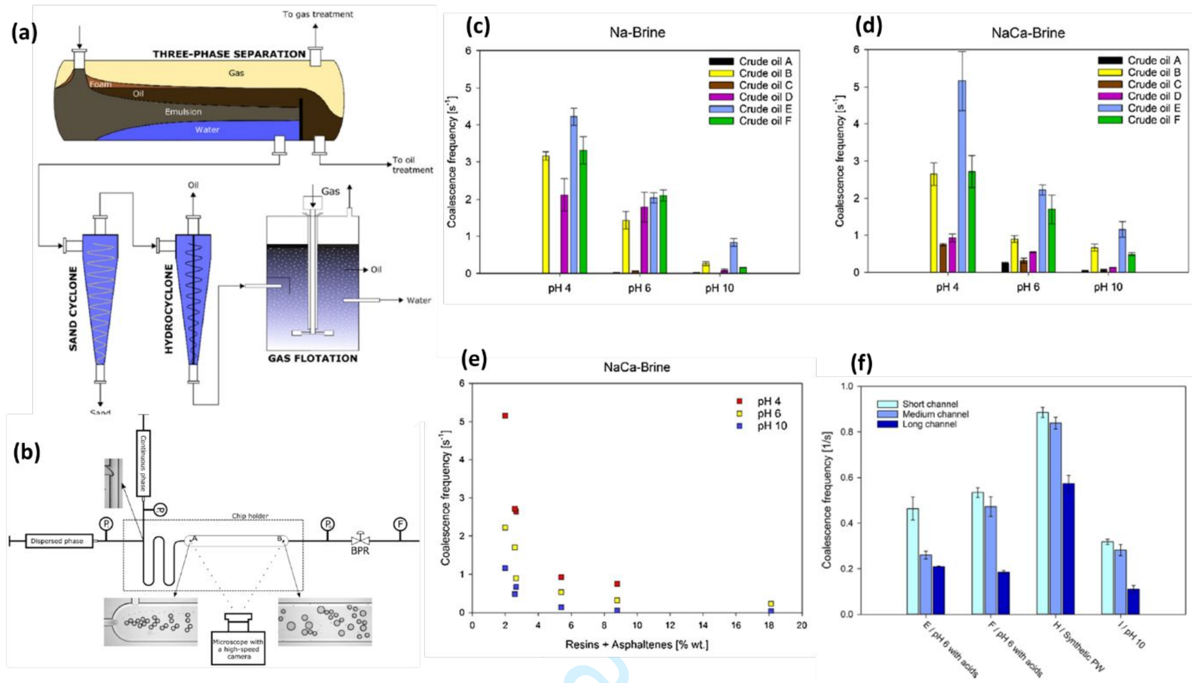

Figure 3. (a) Schematic of produced water treatment process, (b) Schematic of microfluidic setup for emulsion generation, (c) Coalescence frequencies of diluted crude oils in Na-Brine (only NaCl) and (d) NaCa-Brine (a mixture of NaCl and $CaCl_2$) at three different pH values, (e) Coalescence frequencies of diluted crude oils as a function of the sum of resins and asphaltenes for different crude oils. The widths of inlet channels and coalescence chamber are 100 µm and 500 µm, respectively. The depth of all channels is 45 µm. Panels a-e reprinted with permission from ref[13]. Copyright 2018 Elsevier. (f) Coalescence frequencies of crude oil droplets under different experimental conditions as a function of aging time. Panel f reprinted with permission from ref[42]. Copyright 2019 American Chemical Society.

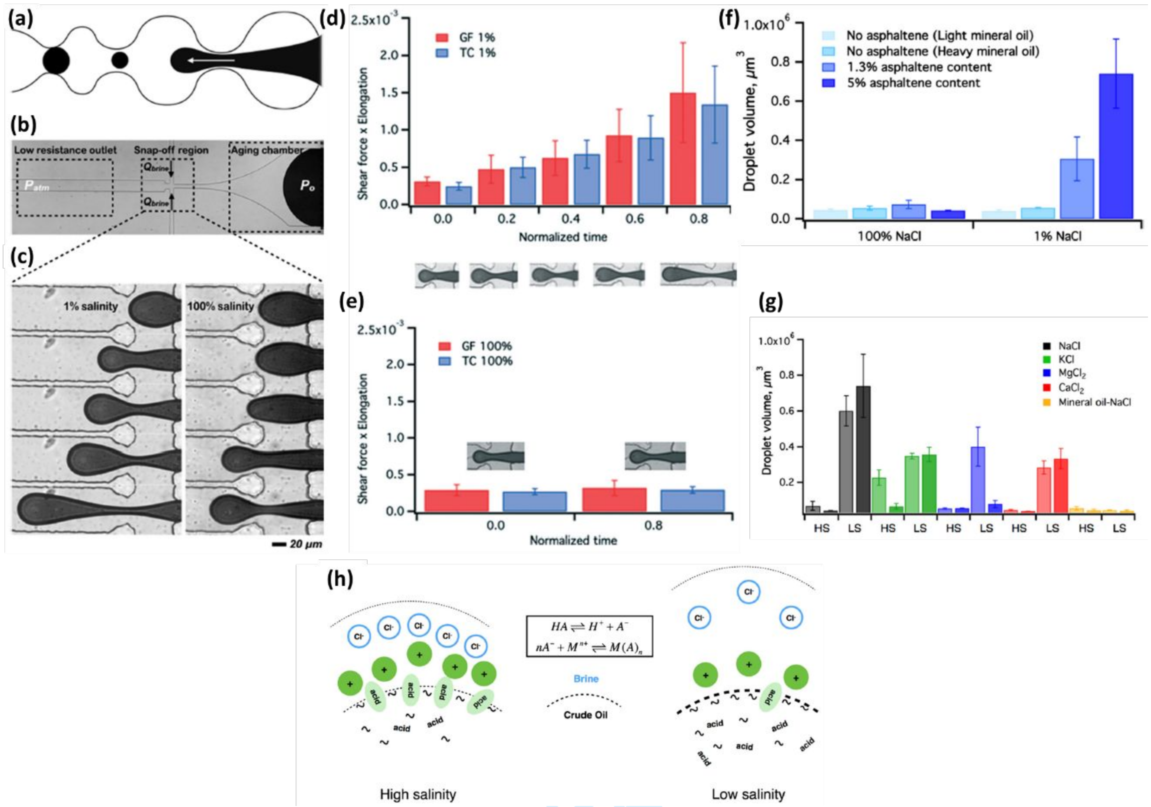

Figure 4. (a) Schematic of snap-off in a porous media; (b) Photograph of flow-focusing microfluidic chip to examine the evolution of interfacial elasticity and their effect on the snap-off. The dark liquid represents the oil phase which is aged against transparent brine; (c) Drop formation and evolution of snap-off for crude oil against both low and high salinity brines. The height of rectangular channel is 20 µm. (d) Normalized shear force during snap-off process obtained via computational fluid dynamics for two different crude oils sourced aged vs. low salinity brine (e) and high salinity brine. Panels a-e reprinted with permission from ref[48]. Copyright 2016 Royal Society of Chemistry. (f) Droplet size as a function of asphaltene content for different oils aged against NaCl brine under low and high salinity conditions (100% salinity=666.94 mmolal, 1% salinity=6.67 mmolal); (g) Droplet size vs. different brine compositions under: (i) non-aging (light bars) and (ii) aging (solid bars) conditions ("HS" and "LS" represent low and high salinity, respectively); and (h) Schematic of the proposed mechanism showing the competition between acids and asphaltene molecules and their possible effects on the interfacial properties under low and high salinity conditions for both non-aging and aging interfaces. Possible acid dissociation and complexation with metal cations are depicted in the solid box. "~" is the asphaltene molecules and "acid" shaded with green demonstrates complexation with metal cations. The bold dashed line in black is representative of interface with enhanced elasticity. Panels f-h reprinted with permission from ref[49]. Copyright 2019 Elsevier.